Proceedings of the 17th World Congress
The International Federation of Automatic Control
Seoul, Korea, July 6-11, 2008

An Adaptive Sensor Fusion Method with Applications in Integrated Navigation

Dah-Jing Jwo*. Tsu-Pin Weng **

** Department of Communications, Navigation and Control Engineering*
National Taiwan Ocean University, Keelung 202-24, Taiwan
(e-mail: djjwo@mail.ntou.edu.tw)
*** EverMore Technology Inc., Hsinchu, Taiwan*
(e-mail:bibby@emt.com.tw)

Abstract: The Kalman filter (KF) is a form of optimal estimator characterized by recursive evaluation, which has been widely applied to the navigation sensor fusion. The adaptive algorithm is one of the approaches to prevent divergence problem of the Kalman filter when precise knowledge on the system models is not available. Two popular types of adaptive Kalman filter are the innovation-based adaptive estimation (IAE) approach and the adaptive fading Kalman filter (AFKF) approach. In this paper, an approach involving the concept of the two methods is proposed. The method is a synergy of the IAE and AFKF approaches. The ratio of the actual innovation covariance based on the sampled sequence to the theoretical innovation covariance is employed for dynamically tuning two filter parameters: fading factors and measurement noise scaling factors. The method has the merits of good computational efficiency and numerical stability. The matrices in the KF loop are able to remain positive definitive. Navigation sensor fusion using the proposed scheme applied to the loosely-coupled GPS/INS integration will be demonstrated.

1. INTRODUCTION

The Kalman filter (KF) (Brown and Hwang, 1997, Gelb, 1974) not only works well in practice, but also it is theoretically attractive since it has been shown to be the filter that minimizes the variance of the estimation mean square error (MSE). Nevertheless, the fact that KF highly depends on a predefined dynamics model forms a major drawback. The case that theoretical behavior of a filter and its actual behavior do not agree may lead to divergence problems. For example, if the Kalman filter is provided with information that the process behaves a certain way, whereas, in fact, it behaves a different way, the filter will continually intend to fit an incorrect process signal. In various circumstances, the availability of a precisely known model is unrealistic due to the fact that in the modeling step, some phenomena are disregarded and a way to take them into account is to consider a nominal model affected by uncertainty.

To fulfill the requirement of achieving the filter optimality or to preventing divergence problem of Kalman filter, the so-called adaptive Kalman filter (AKF) approach has been one of the promising strategies for dynamically adjusting the parameters of the supposedly optimum filter based on the estimates of the unknown parameters for on-line estimation of motion as well as the signal and noise statistics available data. Two popular types of the adaptive Kalman filter algorithms include the innovation-based adaptive estimation (IAE) approach (Ding, et al., 2007; Mehra, 1971, 1972; Mohamed and Schwarz, 1999; Hide et al., 2003) and the adaptive fading Kalman filter (AFKF) approach (Xia et al., 1994), which is a type of covariance scaling method. The AFKF incorporates suboptimal fading factors as a multiplier to enhance the influence of innovation information for improving the tracking capability in high dynamic maneuvering.

The Global Positioning System (GPS) (Brown and Hwang, 1997) and inertial navigation systems (INS) (Farrell, 1998) have complementary operational characteristics and the synergy of both systems has been widely explored. GPS is capable of providing accurate position information. Unfortunately, the data is prone to jamming or being lost due to the limitations of electromagnetic waves, which form the fundamental of their operation. The system is not able to work properly in the areas due to signal blockage and attenuation that may deteriorate the overall positioning accuracy. The INS is a self-contained system that integrates three acceleration components and three angular velocity components with respect to time and transforms them into the navigation frame to deliver position, velocity and attitude components. The three orthogonal linear accelerations are continuously measured through three-axis accelerometers while three gyroscopes sensors monitor the three orthogonal angular rates in an inertial frame of reference. For short time intervals, the integration with respect to time of the linear acceleration and angular velocity monitored by the INS results in an accurate velocity, position and attitude. However, the error in position coordinates increase unboundedly as a function of time. The GPS/INS integration is the adequate solution to provide a navigation system that has superior performance in comparison with either a GPS or an INS stand-alone system. The integration is typically carried out through Kalman filter.

2. KALMAN FILTER AND INNOVATION SEQUENCE

The process model and measurement model are represented as

$$\mathbf{x}_{k+1} = \mathbf{\Phi}_k \mathbf{x}_k + \mathbf{G}_k \mathbf{w}_k \tag{1a}$$

$$\mathbf{z}_k = \mathbf{H}_k \mathbf{x}_k + \mathbf{v}_k \tag{1b}$$

where the state vector $\mathbf{x}_k \in \Re^n$, process noise vector $\mathbf{w}_k \in \Re^n$, measurement vector $\mathbf{z}_k \in \Re^m$, and measurement noise vector $\mathbf{v}_k \in \Re^m$. In Equation (1), both the vectors $\mathbf{w}_k$ and $\mathbf{v}_k$ are zero mean Gaussian white sequences having zero crosscorrelation with each other:

$$\mathbf{E}[\mathbf{w}_k \mathbf{w}_i^{\mathrm{T}}] = \begin{cases} \mathbf{Q}_k, & i = k \\ 0, & i \neq k \end{cases}; \ \mathbf{E}[\mathbf{v}_k \mathbf{v}_i^{\mathrm{T}}] = \begin{cases} \mathbf{R}_k, & i = k \\ 0, & i \neq k \end{cases};$$

$$\mathbf{E}[\mathbf{w}_k \mathbf{v}_i^{\mathrm{T}}] = \mathbf{0} \qquad \textit{for all } i \textit{ and } k \tag{2}$$

where $\mathbf{Q}_k$ is the process noise covariance matrix, $\mathbf{R}_k$ is the measurement noise covariance matrix, $\mathbf{\Phi}_k = e^{\mathbf{F}\Delta t}$ is the state transition matrix, and Δt is the sampling interval, $E[\cdot]$ represents expectation, and superscript "T" denotes matrix transpose. The discrete-time Kalman filter algorithm is summarized as follow:

- Prediction steps/time update equations:

$$\hat{\mathbf{x}}_{k+1}^- = \mathbf{\Phi}_k \hat{\mathbf{x}}_k \tag{3}$$

$$\mathbf{P}_{k+1}^- = \mathbf{\Phi}_k \mathbf{P}_k \mathbf{\Phi}_k^{\mathrm{T}} + \mathbf{Q}_k \tag{4}$$

- Correction steps/measurement update equations:

$$\mathbf{K}_k = \mathbf{P}_k^- \mathbf{H}_k^{\mathrm{T}} [\mathbf{H}_k \mathbf{P}_k^- \mathbf{H}_k^{\mathrm{T}} + \mathbf{R}_k]^{-1} \tag{5}$$

$$\hat{\mathbf{x}}_k = \hat{\mathbf{x}}_k^- + \mathbf{K}_k [\mathbf{z}_k - \mathbf{H}_k \hat{\mathbf{x}}_k^-] \tag{6}$$

$$\mathbf{P}_k = [\mathbf{I} - \mathbf{K}_k \mathbf{H}_k] \mathbf{P}_k^- \tag{7}$$

Equations (3)-(4) are the time update equations of the algorithm from step k to step $k+1$, and Equations (5)-(7) are the measurement update equations. These equations incorporate a measurement value into *a priori* estimation to obtain an improved *a posteriori* estimation.

From the incoming measurement $\mathbf{z}_k$ and the optimal prediction $\hat{\mathbf{x}}_k^-$ obtained in the previous step, the innovations sequence is defined as

$$\boldsymbol{\upsilon}_k = \mathbf{z}_k - \hat{\mathbf{z}}_k^- \tag{8}$$

The innovation reflects the discrepancy between the predicted measurement and the actual measurement. It represents the additional information available to the filter as a consequence of the new observation $\mathbf{z}_k$. Substituting the measurement model Equation (1b) into Equation (8) gives

$$\boldsymbol{\upsilon}_k = \mathbf{H}_k (\mathbf{x}_k - \hat{\mathbf{x}}_k^-) + \mathbf{v}_k \tag{9}$$

An innovation of zero indicates that the two are in complete agreement. The corresponding error mean of an unbiased estimator is zero. By taking variances on both sides, the theoretical covariance matrix of the innovation sequence is given by

$$\mathbf{C}_{\upsilon_k} = E[\boldsymbol{\upsilon}_k \boldsymbol{\upsilon}_k^{\mathrm{T}}] = \mathbf{H}_k \mathbf{P}_k^- \mathbf{H}_k^{\mathrm{T}} + \mathbf{R}_k \tag{10}$$

Defining $\hat{\mathbf{C}}_{\upsilon_k}$ as the statistical sample variance estimate of $\mathbf{C}_{\upsilon_k}$, matrix $\hat{\mathbf{C}}_{\upsilon_k}$ can be computed through averaging inside a moving estimation window of size N

$$\hat{\mathbf{C}}_{\upsilon_k} = \frac{1}{N} \sum_{j=j_0}^{k} \boldsymbol{\upsilon}_j \boldsymbol{\upsilon}_j^{\mathrm{T}} \tag{11}$$

where N is the number of samples (usually referred to the window size); $j_0 = k - N + 1$ is the first sample inside the estimation window. The window size N is chosen empirically (The values between 10 and 30 are commonly used.) to give some statistical smoothing. More detailed discussion is referred to Gelb (1974), Brown & Hwang (1997), and Mohamed & Schwarz (1999).

3. THE PROPOSED ADAPTIVE SENSOR FUSION STRATEGY

A new strategy for tuning the filter parameters is presented. The conventional KF approach is coupled with the adaptive tuning system (ATS) for providing two system parameters: fading factor and noise covariance scaling factor. In the ATS mechanism, both adaptations on process noise covariance (referred to P-adaptation herein) and on measurement noise covariance (referred to R-adaptation herein) are involved. The idea is based on the concept that when the filter achieves estimation optimality, the actual innovation covariance based on the sampled sequence and the theoretical innovation covariance should be equal. In other words, the ratio between the two should approach unity.

3.1 Adaptation on process noise covariance

The idea of fading Kalman filtering is to apply a factor matrix to the predicted covariance matrix to deliberately increase the variance of the predicted state vector. To account for the uncertainty, the covariance matrix needs to be updated, through the following way. The new $\overline{\mathbf{P}}_k^-$ can be obtained by multiplying $\mathbf{P}_k^-$ by the factor $\boldsymbol{\lambda}_P$:

$$\overline{\mathbf{P}}_k^- = \boldsymbol{\lambda}_P \mathbf{P}_k^- \tag{12}$$

and the corresponding Kalman gain is given by

$$\overline{\mathbf{K}}_k = \overline{\mathbf{P}}_k^- \mathbf{H}_k^{\mathrm{T}} [\mathbf{H}_k \overline{\mathbf{P}}_k^- \mathbf{H}_k^{\mathrm{T}} + \overline{\mathbf{R}}_k]^{-1} \tag{13a}$$

If representing the new variable $\overline{\mathbf{R}}_k = \boldsymbol{\lambda}_R \mathbf{R}_k$, we have

$$\overline{\mathbf{K}}_k = \overline{\mathbf{P}}_k^- \mathbf{H}_k^{\mathrm{T}} [\mathbf{H}_k \overline{\mathbf{P}}_k^- \mathbf{H}_k^{\mathrm{T}} + \boldsymbol{\lambda}_R \mathbf{R}_k]^{-1} \tag{13b}$$

From Equation (13b), it can be seen that the change of covariance is essentially governed by two of the parameters: $\overline{\mathbf{P}}_k^-$ and $\mathbf{R}_k$. In addition, the covariance matrix at the measurement update stage, from Equation (7), can be written as

$$\overline{\mathbf{P}}_k = [\mathbf{I} - \overline{\mathbf{K}}_k \mathbf{H}_k] \overline{\mathbf{P}}_k^- \tag{14a}$$

and

$$\overline{\mathbf{P}}_k = \boldsymbol{\lambda}_P[\mathbf{I} - \overline{\mathbf{K}}_k\mathbf{H}_k]\mathbf{P}_k^- \tag{14b}$$

Furthermore, based on the relationship given by Equation (12), the covariance matrix at the prediction stage (i.e., Equation (4)) is given by

$$\overline{\mathbf{P}}_{k+1}^- = \boldsymbol{\Phi}_k\overline{\mathbf{P}}_k\boldsymbol{\Phi}_k^{\mathrm{T}} + \mathbf{Q}_k \tag{15}$$

or, alternatively

$$\overline{\mathbf{P}}_{k+1}^- = \boldsymbol{\lambda}_P\boldsymbol{\Phi}_k\mathbf{P}_k\boldsymbol{\Phi}_k^{\mathrm{T}} + \mathbf{Q}_k \tag{16a}$$

On the other hand, the covariance matrix can also be approximated by

$$\overline{\mathbf{P}}_{k+1}^- = \boldsymbol{\lambda}_P\mathbf{P}_{k+1}^- = \boldsymbol{\lambda}_P(\boldsymbol{\Phi}_k\mathbf{P}_k\boldsymbol{\Phi}_k^T + \mathbf{Q}_k) \tag{16b}$$

where $\boldsymbol{\lambda}_P = diag(\lambda_1, \lambda_2 \ldots, \lambda_m)$. The main difference between various adaptive fading algorithms is essentially on the calculation of scale factor $\boldsymbol{\lambda}_P$. One approach is to assign the scale factors as constants. When $\lambda_i \le 1$ ($i = 1,2,\ldots,m$), the filtering is in a steady state processing while $\lambda_i > 1$, the filtering may tend to be unstable. For the case $\lambda_i = 1$, it deteriorates to the standard Kalman filter. There are some drawbacks with constant factors, e.g., as the filtering proceeds, the precision of the filtering will decrease because the effects of old data tend to become less and less. The ideal way is to use time varying factors that are determined according to the dynamic and observation model accuracy. When there is deviation due to the changes of covariance and measurement noise, the corresponding innovation covariance matrix can be rewritten as:

$$\overline{\mathbf{C}}_{\upsilon_k} = \mathbf{H}_k\overline{\mathbf{P}}_k^-\mathbf{H}_k^{\mathrm{T}} + \overline{\mathbf{R}}_k$$

and

$$\overline{\mathbf{C}}_{\upsilon_k} = \boldsymbol{\lambda}_P\mathbf{H}_k\mathbf{P}_k^-\mathbf{H}_k^{\mathrm{T}} + \boldsymbol{\lambda}_R\mathbf{R}_k \tag{17}$$

To enhance the tracking capability, the time-varying suboptimal scaling factor is incorporated, for on-line tuning the covariance of the predicted state, which adjusts the filter gain, and accordingly the improved version of AFKF is obtained. The optimum fading factors can be calculated through the single factor:

$$\lambda_i = (\boldsymbol{\lambda}_P)_{ii} = \max\left\{1, \frac{tr(\hat{\mathbf{C}}_{\upsilon_k})}{tr(\mathbf{C}_{\upsilon_k})}\right\},\ i = 1,2\ldots,m \tag{18}$$

where $tr[\cdot]$ is the trace of matrix; $\lambda_i \ge 1$, is a scaling factor. Increasing λ_i will improve tracking performance.

3.2 Adaptation on measurement noise covariance

As the strength of measurement noise changes with the environment, incorporation of the fading factor only is not able to restrain the expected estimation accuracy. For resolving these problems, the ATS needs a mechanism for R-adaptation in addition to P-adaptation, to adjust the noise strengths and improve the filter estimation performance.

A parameter which represents the ratio of the actual innovation covariance based on the sampled sequence and the theoretical innovation covariance matrices can be defined as one of the following methods:

(a) Single factor

$$\lambda_j = (\boldsymbol{\lambda}_R)_{jj} = \frac{tr(\hat{\mathbf{C}}_{\upsilon_k})}{tr(\mathbf{C}_{\upsilon_k})}\ ,\ j = 1,2\ldots,n \tag{19a}$$

(b) Multiple factors

$$\lambda_j = \frac{(\hat{\mathbf{C}}_{\upsilon_k})_{jj}}{(\mathbf{C}_{\upsilon_k})_{jj}}\ ,\ j = 1,2\ldots,n \tag{19b}$$

It should be noted that from Equation (17) that increasing $\mathbf{R}_k$ will lead to increasing $\mathbf{C}_{\upsilon_k}$, and vice versa. This means that time-varying $\mathbf{R}_k$ leads to time-varying $\mathbf{C}_{\upsilon_k}$. The value of $\boldsymbol{\lambda}_R$ is introduced in order to reduce the discrepancies between $\mathbf{C}_{\upsilon_k}$ and $\mathbf{R}_k$. The adaptation can be implemented through the simple relation:

$$\overline{\mathbf{R}}_k = \boldsymbol{\lambda}_R\mathbf{R}_k \tag{20}$$

Further detail regarding the adaptive tuning loop is illustrated by the flow charts shown in Figs.1 and 2, where two architectures are presented. Fig.1 shows the System architecture #1 and Fig.2 shows the System architecture #2, respectively. In Fig.1, the flow chart contains two portions, for which the block indicated by the dot lines is the adaptive tuning system (ATS) for tuning the values of both P and R parameters; in Fig.2, the flow chart contains three portions, for which the two blocks indicated by the dot lines represent the R-adaptation loop and P-adaptation loop, respectively.

An important remark needs to be pointed out. When the System architecture #1 is employed, only one window size is needed. It can be seen that the measurement noise covariance of the innovation covariance matrix hasn't been updated when performing the fading factor calculation. In the System architecture #2, the latest information of the measurement noise strength has already been available when performing the fading factor calculation. However, one should notice that utilization of the 'old' (i.e., before R-adaptation) information is required. Otherwise, unreliable result may occur since the deviation of the innovation covariance matrix due to the measurement noise can not be correctly detected. One strategy for avoiding this problem can be done by using two different window sizes, one for R-adaptation loop and the other for P-adaptation loop.

4. SIMULATION EXPERIMENTS AND ANALYSIS

Simulation experiments have been carried out to evaluate the performance of the proposed approach in comparison with the conventional methods for GPS/INS navigation processing. The loosely-coupled architecture is selected for demonstration, as shown in Fig.3. The computer codes were constructed using the Matlab® 6.5 version software. The commercial software Satellite Navigation (SATNAV) Toolbox by GPSoft LLC was employed for generating the satellite positions and pseudoranges. The satellite constellation was simulated and the error sources corrupting GPS measurements include ionospheric delay, tropospheric delay, receiver noise and multipath. Assume that the

differential GPS mode is used and most of the errors can be corrected, but the multipath and receiver thermal noise cannot be eliminated.

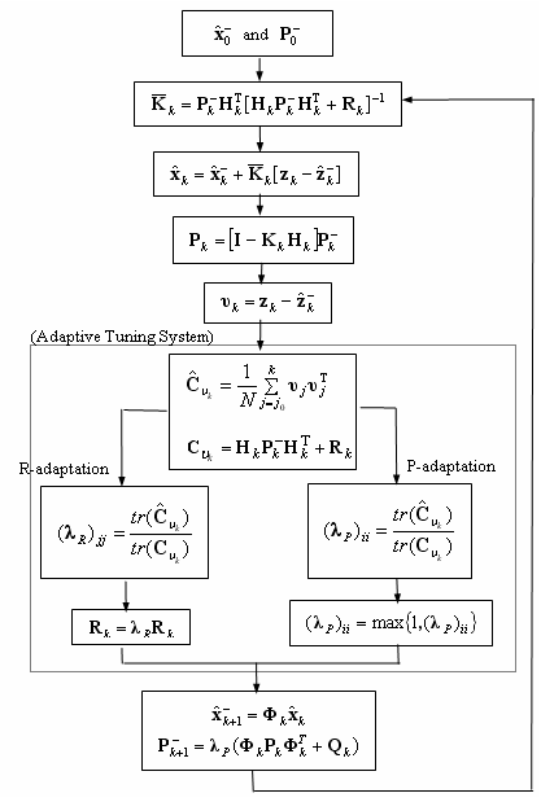

Fig.1. Flow chart of the proposed AKF method - System architecture #1.

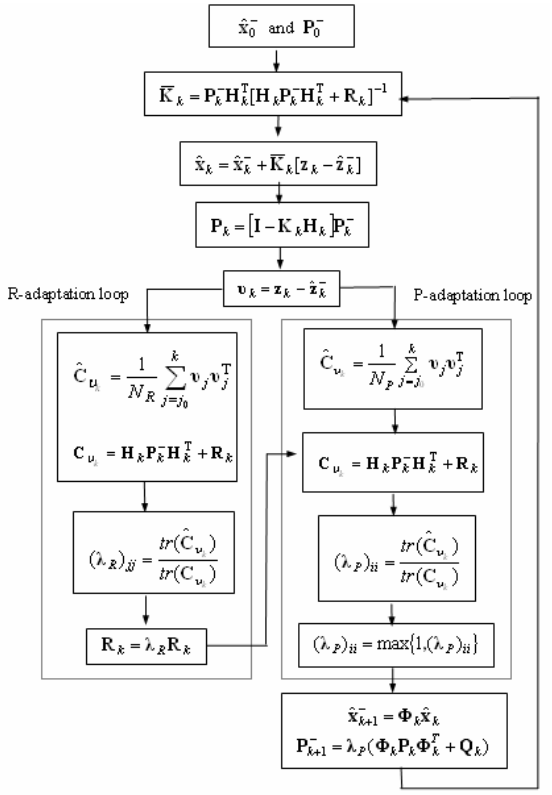

Fig.2. Flow chart of the proposed AKF method - System architecture #2.

The differential equations describing the two-dimensional inertial navigation state are (Farrell, 1998):

$$\begin{bmatrix}\dot{n}\\ \dot{e}\\ \dot{v}_n\\ \dot{v}_e\\ \dot{\psi}\end{bmatrix} = \begin{bmatrix}v_n\\ v_e\\ a_n\\ a_e\\ \omega_r\end{bmatrix} = \begin{bmatrix}v_n\\ v_e\\ \cos(\psi)a_u - \sin(\psi)a_v\\ \sin(\psi)a_u + \cos(\psi)a_v\\ \omega_r\end{bmatrix} \tag{21}$$

where $[\,a_u\,,\,a_v\,]$ are the measured accelerations in the body frame, ω_r is the measured yaw rate in the body frame. It is usually difficult to set a certain stochastic model for each inertial sensor that works efficiently at all environments and reflects the long-term behavior of sensor errors. The following set of linearized equations is used

$$\begin{bmatrix}\delta\dot{n}\\ \delta\dot{e}\\ \delta\dot{v}_n\\ \delta\dot{v}_e\\ \delta\dot{\psi}\end{bmatrix} = \begin{bmatrix}0&0&1&0&0\\ 0&0&0&1&0\\ 0&0&0&0&0\\ 0&0&0&0&0\\ 0&0&0&0&0\end{bmatrix}\begin{bmatrix}\delta n\\ \delta e\\ \delta v_n\\ \delta v_e\\ \delta\psi\end{bmatrix} + \begin{bmatrix}0\\ 0\\ w_n\\ w_e\\ w_\psi\end{bmatrix} \tag{22}$$

which will be utilized in the integration Kalman filter as the inertial error model. In Equation (22), δn and δe represent the east, and north position errors; δv_n and δv_e represent the east, and north velocity errors; and $\delta\psi$ represent yaw angle, respectively. The measurement model is given by

$$\begin{bmatrix}\delta n\\ \delta e\end{bmatrix} = \begin{bmatrix}n_{INS}\\ e_{INS}\end{bmatrix} - \begin{bmatrix}n_{GPS}\\ e_{GPS}\end{bmatrix} = \begin{bmatrix}1&0&0&0&0\\ 0&1&0&0&0\end{bmatrix}\begin{bmatrix}\delta n\\ \delta e\\ \delta v_n\\ \delta v_e\\ \delta\psi\end{bmatrix} + \begin{bmatrix}v_n\\ v_e\end{bmatrix} \tag{23}$$

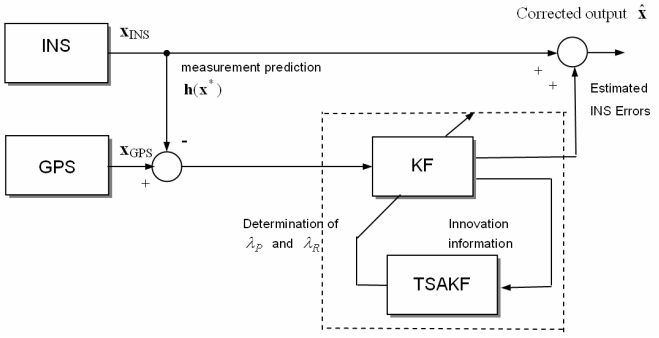

Fig.3. GPS/INS navigation processing using the proposed AKF.

Experiment was conducted on a simulated vehicle trajectory originating from the (0,0) m location. The simulated outputs for the accelerometers and gyroscope are shown in Fig.4. The trajectory of the vehicle can be approximately divided into two categories according to the dynamic characteristics. The vehicle was simulated to conduct constant-velocity straight-line during the three time intervals, 0-300, 901-1200 and 1501-1800s, all at a speed of 10π m/s. Furthermore, it conducted counterclockwise circular motion with radius 3000 meters during 301-900, and 1201-1500s where high dynamic

maneuvering is involved. The following parameters were used: window size $N_p = 15$ $N_R = 20$; the values of noise standard deviation are 1e-3 m/s^2 for accelerometers and gyroscopes. Trajectory for the simulated vehicle (solid) and the unaided INS derived position (dashed) is shown in Fig.5.

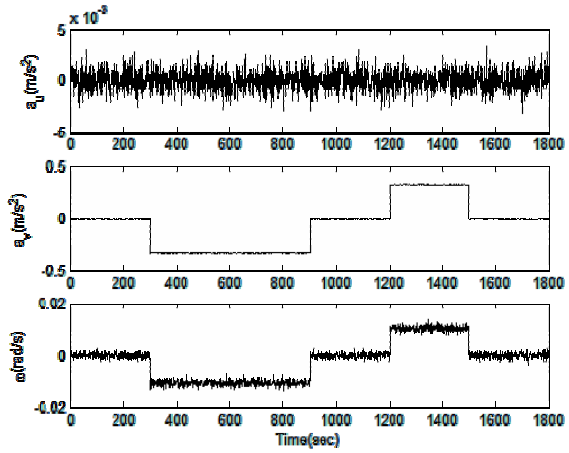

Fig. 4. Simulated outputs for the accelerometers and gyroscope.

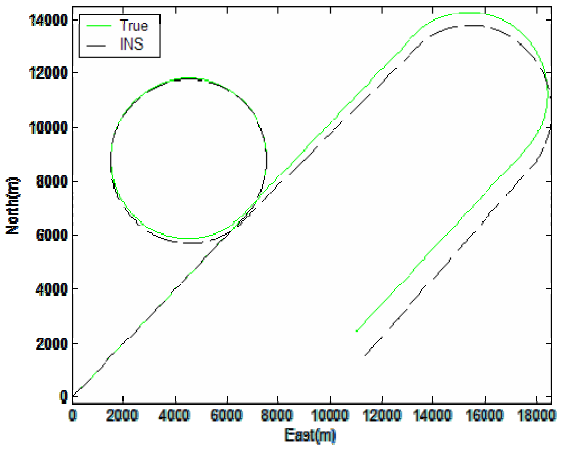

Fig. 5. Trajectory for the simulated vehicle (solid) and the INS derived position (dashed).

In the real world, the measurement will normally be changing in addition to the change of process noise or dynamic such as maneuvering. In such case, both P-adaptation and R-adaptation tasks need to be implemented. In the following discussion, results will be provided for the case when measurement noise strength is changing in addition to the change of process noise strength. The measurement noise strength is assumed to be changing with variances of the values $r = 4^2 \rightarrow 16^2 \rightarrow 8^2 \rightarrow 3^2$, where the 'arrows $(\rightarrow)$' is employed for indicating the time-varying trajectory of measurement noise statistics. That is, it is assumed that the measure noise strength is changing during the four time intervals: 0-450s ($N(0,4^2)$), 451-900s ($N(0,16^2)$), 901-1350s ($N(0,8^2)$), and 1351-1800s ($N(0,3^2)$). However, the internal measurement noise covariance matrix $\mathbf{R}_k$ is set unchanged all the time in simulation, which uses $r_j \sim N(0,3^2)$, $j = 1,2\ldots,n$, at all the time intervals.

Fig.6 shows the east and north components of navigation errors and the 1-σ bound based on the method without adaptation on measurement noise covariance matrix. It can be seen that the correct P information with incorrect R information (referred to partial adaptation herein) seriously deteriorates the estimation result. Fig.7 provides the east and north components of navigation errors and the 1-σ bound based on the proposed method (referred to full adaptation herein, i.e., adaptation on both estimation covariance and measurement noise covariance matrices are applied). The estimation accuracy has now been substantially improved. It can also been seen that the measurement noise strength has been accurately estimated, as shown in Fig.8.

It should also be mentioned that the requirement $(\lambda_P)_{ii} \geq 1$ is critical. Example for illustration is given in Figs.9 and 10. Fig.9 gives the navigation errors and the 1-σ bound when the threshold setting is not incorporated. The corresponding reference (true) and calculated standard deviations when the threshold setting is not incorporated is provided in Fig.10. It is not surprising that the navigation accuracy has been seriously degraded due to the inaccurate estimation of measurement noise statistics.

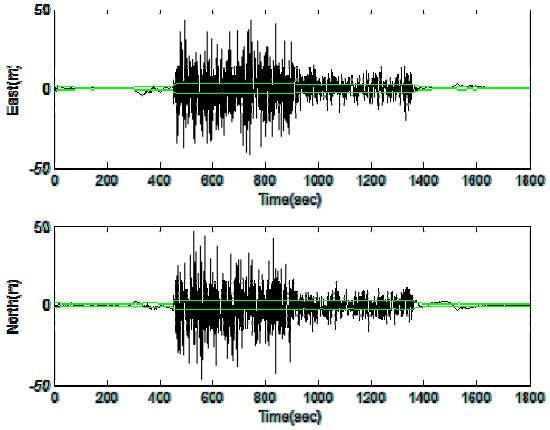

Fig.6. East and north components of navigation errors and the 1-σ bound based on the method without adaptation on measurement noise.

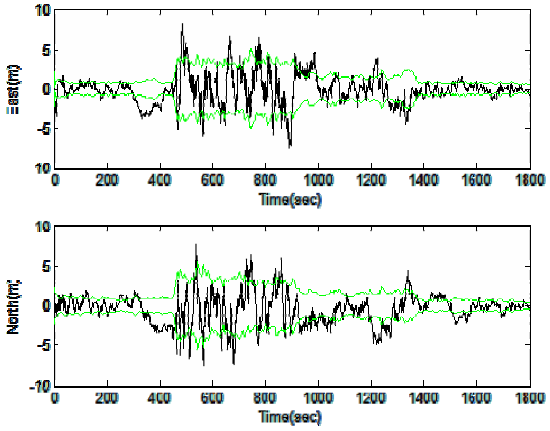

Fig.7. East and north components of navigation errors and the 1-σ bound based on the proposed method (with full adaptation).

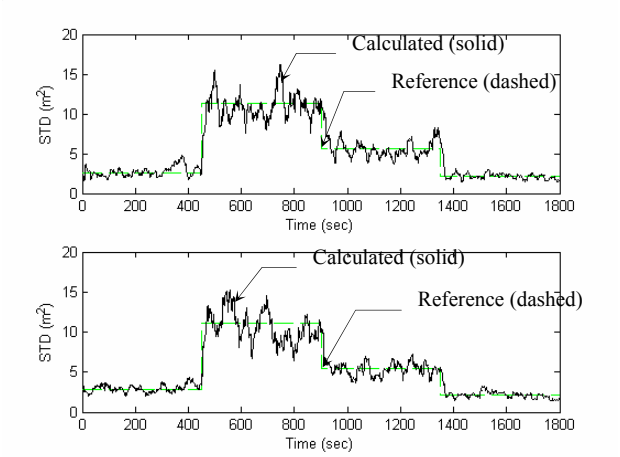

Fig.8. Reference (true) and calculated standard deviations for the east (top) and north (bottom) components of the measurement noise variance values.

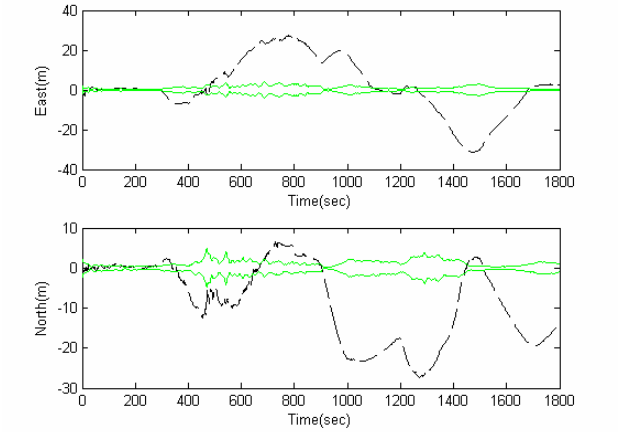

Fig.9. East and north components of navigation errors and the 1-σ bound based on the proposed method when the threshold setting is not incorporated.

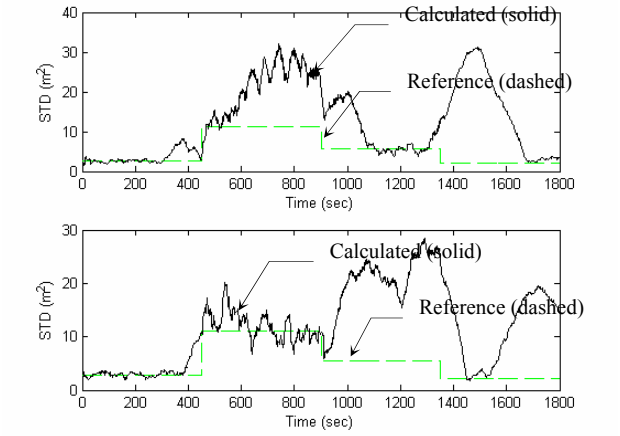

Fig.10. Reference (true) and calculated standard deviations for the east and north components of the measurement noise variance values when the threshold setting is not incorporated.

5. CONCLUSIONS

This paper has proposed a new strategy of adaptive Kalman filter approach and provided an illustrative example for integrated navigation application. The conventional KF approach is coupled by the adaptive tuning system (ATS), which gives two system parameters: the fading factor and measurement noise covariance scaling factor. The ATS has been employed as a mechanism for timely detecting the dynamical and environmental changes and implementing the on-line parameter tuning by monitoring the innovation information so as to maintain good tracking capability and estimation accuracy. Unlike some of the conventional AKF method, the proposed method has the merits of good computational efficiency and numerical stability. The matrices in the KF loop are able to remain positive definitive. Remarks to be noted for using the method is made, such as: (1) The window sizes can be set different, to avoid the filter degradation/divergence; (2) The fading factors $(\boldsymbol{\lambda}_P)_{ii}$ should be always larger than one while $(\boldsymbol{\lambda}_R)_{jj}$ does not have such limitation. Simulation experiments for navigation sensor fusion have been provided to illustrate the accessibility. The accuracy improvement based on the proposed AKF method has demonstrated substantial improvement in both navigational accuracy and tracking capability.

ACKNOWLEDGEMENTS

This work has been supported in part by the National Science Council of the Republic of China under grant no. NSC 96-2221-E-019-007.

REFERENCES

Brown, R., and Hwang, P. (1997). *Introduction to Random Signals and Applied Kalman Filtering*. John Wiley & Sons, New York.

Ding, W., Wang, J., and Rizos, C. (2007). Improving Adaptive Kalman Estimation in GPS/INS Integration. *Journal of Navigation,* **60**, 517-529.

Mehra, R. K. (1971). On-line identification of linear dynamic systems with applications to Kalman filtering, *IEEE Trans. Automat. Contr.*, **AC-16**, 12-21.

Mehra, R. K. (1972). Approaches to adaptive filtering, *IEEE Trans. Automat. Contr.*, **AC-17**, 693-698.

Mohamed, A. H. and Schwarz, K. P. (1999). Adaptive Kalman filtering for INS/GPS, *Journal of Geodesy*, **73**, 193-203.

Hide, C, Moore, T., and Smith, M. (2003). Adaptive Kalman filtering for low cost INS/GPS, *Journal of Navigation*, **56**, 143-152.

Gelb, A. (1974). *Applied Optimal Estimation*. M. I. T. Press, MA.

Farrell, J. (1998). *The Global Positioning System and Inertial Navigation*, McCraw-Hill professional.

Xia, Q., Rao, M., Ying, Y., and Shen, X. (1994). Adaptive fading Kalman filter with an application, *Automatica*, **30**, 1333-1338.